

1		
		<u>SUPPLEMENTARY MATERIAL</u>
2		TABLE OF CONTENTS
3	1.- Online Supplementary Methods	2
4	1.1 Study cohort	2
5	1.2 Genotyping and quality control	2
6	1.3 Imputation	3
7	1.4 Association testing and meta-analysis	4
8	1.5 Heritability estimation	4
9	1.6 Clinical subtype specificity	4
10	1.7 Statistical fine-mapping of JIA-associated loci	5
11	1.8 Functional annotation enrichment analysis	5
12	1.9 Gene prioritisation with eQTL	6
13	1.10 Chromatin interaction analysis in human B and T cell types	6
14	2.- Supplementary Figure Legends	8
15	3.- Supplementary Figures	9
16	4.- Supplementary References.....	13
17		

18 **1. ONLINE SUPPLEMENTARY METHODS**

19 **1.1 Study cohort**

20 A total of 4,520 UK juvenile idiopathic arthritis (JIA) samples were recruited from
21 multiple sources: the British Society for Paediatric and Adolescent Rheumatology (BSPAR)
22 National Repository of JIA, the Childhood Arthritis Prospective Study (CAPS), the
23 Childhood Arthritis Response to Medication Study (CHARMS), the UK JIA Genetics
24 Consortium (UKJIAGC), The Biologics for Children with Rheumatic Diseases (BCRD)
25 study, and the British Society for Paediatric and Adolescent Rheumatology Etanercept Cohort
26 Study (BSPAR-ETN), a group of UK cases with long-standing JIA as described
27 previously[1]. JIA participants were recruited with ethical approval and provided informed
28 consent, including from the North West Multi-centre for Research Ethics Committee
29 (MREC:02/8/104 and MREC:99/8/84), West Midlands Multi-centre Research Ethics
30 Committee (MREC:02/7/106), North West Research Ethics Committee (REC:09/H1008/137)
31 and the NHS Research Ethics Committee (REC:05/Q0508/95). JIA cases were classified
32 according to the International League of Associations for Rheumatology (ILAR) criteria[2]
33 (Supplementary Table 1). Healthy controls data on 9,965 individuals was obtained from the
34 UK Household Longitudinal Study (<https://www.understandingsociety.ac.uk/>) accessed via
35 the European Genome-phenome Archive.

36 **1.2 Genotyping and quality control**

37 JIA DNA samples were genotyped on the Illumina Infinium CoreExome and Infinium
38 OnmiExpress genotyping arrays in accordance to the manufacturer's instructions. Genotype
39 calling was performed by the GenCall algorithm in the GenomeStudio Data Analysis software
40 platform (Genotyping Module v1.8.4). Preliminary genotype clustering was performed using
41 the default Illumina cluster file to identify poor quality samples (call rate < 0.90). Following
42 exclusion of low-quality samples, automated reclustering was performed to calibrate genotype

43 clusters based on the study samples. Sample-level quality control (QC) was performed based
44 on the following exclusion criteria: final call rate < 0.98, outlier based on autosomal
45 heterozygosity (2 standard deviations from the mean) and discrepancy between genetically
46 inferred sex and database records. Single-nucleotide polymorphisms (SNPs) were excluded if
47 they were non-autosomal, had a call rate < 0.98 or a minor allele frequency (MAF) < 0.01.
48 Healthy controls were genotyped at the Wellcome Trust Sanger Institute using the Illumina
49 Infinium CoreExome genotyping array. Sample and SNP QC was consistent with that
50 described above for JIA case samples.

51 The two datasets were combined retaining the intersection of SNPs. Identity-by-
52 descent was used to identify related individuals (kinship coefficient > 0.0884) across all study
53 samples performed with the KING software package (version 1.9)[3]. For each related pair,
54 the sample with the highest call rate was preferentially retained. Individuals were excluded if
55 they were identified as outliers based on ancestry using principal component analysis (PCA)
56 performed with the flashpca software package (version 2.0) where outliers were identified
57 using aberrant R library (version 1.0)[4,5].

58 The total number of individuals that remained in the final QC-filtered dataset was
59 12,501 (3,305 cases and 9,196 healthy controls).

60 **1.3 Imputation**

61 QC-filtered GWAS dataset was subjected to whole-genome genotype imputation.
62 Prior to imputation, SNPs with ambiguous alleles (C/G and A/T) were excluded and
63 remaining SNPs were aligned to the Haplotype Reference Consortium (HRC) panel (version
64 1.1) using the HRC imputation preparation tool
65 (<https://www.well.ox.ac.uk/~wrayner/tools/>)[6]. Phasing and imputation were performed in
66 the Michigan Imputation server using SHAPEIT2[7] and Minimac3[8] respectively, and HRC

67 panel for reference. Following imputation, SNPs were excluded based on a MAF < 0.01 and
68 imputation quality (r^2) < 0.4.

69 **1.4 Association testing and meta-analysis**

70 Case-control association testing was performed by SNPTEST software package
71 (version 2.5.2) using the score method to account for imputation uncertainty. Three principal
72 components, calculated as described above following exclusion of outliers, were included as
73 covariates to account for any residual population sub-structure. Lambda genomic control
74 (λ_{GC}), corrected for sample size (λ_{1000}), was calculated to test for inflation of test statistics
75 attributable to population stratification not accounted for in the analysis. Any SNP with a p-
76 value < 5×10^{-6} was selected for validation in GWAS summary statistics from an independent
77 dataset of 2,751 JIA cases (oligoarticular arthritis (oligoJIA) and rheumatoid factor (RF)-
78 negative polyarthritis (RF-polyJIA)) and 15,886 controls of European Ancestry[9]. An
79 inverse variance weighted fixed effects meta-analysis was performed using the software
80 package GWAMA (version 2.2.2)[10]. The presence of heterogeneity of odds ratios (ORs)
81 across datasets was evaluated with the test statistics I^2 and Q.

82 **1.5 Heritability estimation**

83 SNP-based heritability estimates were calculated using GCTA based on imputed data
84 for all JIA cases[11]. Imputed SNPs were stratified into linkage disequilibrium (LD) score
85 bins and a genetic relationship matrix (GRM) was calculated separately for each bin followed
86 by restricted maximum likelihood (REML) analysis performed on the multiple GRMs.

87 **1.6 Clinical subtype specificity**

88 The specificity and sharing of JIA susceptibility SNPs across ILAR subtypes was
89 interrogated using Bayesian multinomial logistic regression assuming an additive model
90 implemented in the software package Trinculo (version 0.96) using default correlation priors
91 (0.04) for all index SNPs with p-value < 5×10^{-6} [12]. In addition, we have included previously

92 reported JIA susceptibility SNPs based on analysis of a combined oligoJIA and RF-polyJIA
93 cohort[13]. Trinculo identifies the best disease-specific model, the best sharing model, and
94 estimates the Bayes factor between them at each analysed locus. Model selection was based
95 on comparison of log-Bayes factors where a positive log-Bayes factor for specificity was
96 interpreted as evidence that a particular association is specific to an ILAR subtype and a
97 negative value indicative of sharing across multiple ILAR subtypes. The undifferentiated
98 subtype was not included in this analysis.

99 **1.7 Statistical fine-mapping of JIA-associated loci**

100 The boundaries of independently associated loci were defined by a genetic distance of
101 0.1 centimorgans (cM) upstream and downstream of each lead SNP using HapMap fine-scale
102 recombination rate estimates. Statistical fine-mapping of the association signal within each
103 locus was performed using the FINEMAP software package (version 1.3.1) using the shotgun
104 stochastic search function to identify independent effects using an LD panel of 4,000
105 randomly selected controls from the Understanding Society dataset[14]. The 95% credible
106 SNP sets for each locus were selected on the summation of the posterior inclusion
107 probabilities (PIPs) for the most likely causal SNPs. Any independent effects within each
108 locus identified by the stochastic search approach were verified by conditional and joint
109 analysis using GCTA-COJO with the same LD panel as FINEMAP (version 1.92.4)[15]. All
110 identified credible SNPs were annotated with gene location based on RefSeq transcript and
111 evidence for association with other diseases using data from the GWAS catalogue[16]. Non-
112 synonymous credible SNPs were annotated with the pre-calculated Combined Annotation
113 Dependent Depletion (CADD) raw score and scaled score from dbNSFP (version 3.3a)[17].
114 Annotation was performed with ANNOVAR (version 2019Oct24)[18].

115 **1.8 Functional annotation enrichment analysis**

116 Summary statistics from the association analysis of all ILAR subtypes were tested for
117 enrichment in four categories of annotations based on experimental functional genomic data
118 including gene structure (coding sequence (CDS), 3'UTR and 5'UTR) from the GENCODE
119 Project, binding sites for 165 transcription factors from the ENCODE Project, and enhancers
120 and active promoters for 98 cell types derived from the Roadmap Epigenomics Project[19–
121 21]. Enrichment of JIA associations were tested separately in each annotation using fgwas
122 (version 0.3.6)[22]. A joint model of independent enrichments was identified using a forward
123 selection approach of selecting the most significant annotation and sequentially adding
124 additional significant annotations and retaining those that significantly increase the likelihood
125 of the joint model using cross-validation with penalised likelihood to identify the model with
126 the highest cross-validation likelihood.

127 **1.9 Gene prioritisation with eQTL**

128 Expression quantitative trait locus (eQTL) data for 15 cell types was downloaded from
129 the DICE (Database of Immune Cell Expression, eQTLs and Epigenomics) project
130 website[23]. Cell types consisted of three innate immune cell types (CD14^{high} CD16⁻ classical
131 monocytes, CD14⁻ CD16⁺ non-classical monocytes, CD56^{dim} CD16⁺ natural killer (NK) cells),
132 four adaptive immune cell types that have not encountered cognate antigen in the periphery
133 (naive B cells, naive CD4⁺ T cells, naive CD8⁺ T cells, and naive regulatory T cells [Treg]),
134 six CD4⁺ memory or more differentiated T cell subsets (T_H1, T_H1/17, T_H17, T_H2, follicular
135 helper T cell [T_{fh}], and memory Treg [mTreg]), and two activated cell types (naive CD4⁺ and
136 CD8⁺ T cells that were stimulated *ex vivo*) (description from DICE website [https://dice-
137 database.org/](https://dice-database.org/)). Correlation of susceptibility association signals and gene expression were
138 identified by selecting the top eQTL SNP for each gene in each eQTL dataset and retaining
139 those that were also present in the combined list of all FINEMAP credible SNPs for

140 associated loci. Colocalisation of the susceptibility association and eQTL signals was then
141 confirmed using the coloc R package using approximate Bayes factors[24].

142 **1.10 Chromatin interaction analysis in human B and T cell types**

143 Prioritisation of causal genes was further complemented by the interrogation of
144 chromatin interaction data for SNPs correlated with eQTL signals. H3K27ac HiChIP data in
145 GM12878, primary human naïve T cells (CD4⁺CD45RA⁺CD25⁻CD127^{high}), regulatory T
146 (Treg) cells (CD4⁺CD25⁺CD127^{low}) and T_H17 cells (CD4⁺CD45RA⁻CD25⁻
147 CD127^{high}CCR6⁺CXCR5⁻) were interrogated to identify target genes of JIA-associated
148 regions[25]. In detail, sequencing data for the HiChIP libraries was filtered and the adapters
149 were removed using fastp v0.19.4[26]. Then we mapped the reads to the human reference
150 genome GRCh38 with Hi-C Pro v2.11.0 using default settings[27]. HiChIP-peaks v0.1.1 was
151 used with default settings and false discovery rate (FDR) < 0.01 to identify H3K27ac peaks
152 enriched regions[28]. Identification of significant chromatin loops was performed with
153 FitHiChIP using the following settings: Coverage normalization, stringent background with
154 merging enabled, peaks generated from HiChIP-peaks and 5kb bin size[29]. We explored
155 chromatin interaction profiles of the credible SNPs sets from each locus. To identify the
156 connectivity of credible SNPs to target genes, we subsetted the interactions to those linking a
157 transcription start site (TSS) and SNPs overlapping a H3K27ac HiChIP peak in a 5kb
158 resolution. We also nominated the genes for which the TSS was within 1kb of a credible SNP
159 overlapping an H3K27ac peak as identified from HiChIP data. In addition, we explored
160 chromatin interaction maps obtained by capture Hi-C experiments in GM12878 and Jurkat
161 cell types[30]. Credible SNPs were set as anchor points to identify physical interactions
162 between restriction fragments containing the variants and gene promoters using IRanges and
163 GenomicRanges R packages.

164

165

166 **2. SUPPLEMENTARY FIGURE LEGENDS**

167 **Supplementary Figure 1. Bayesian model selection analysis for ILAR subtype**
168 **specificity of JIA susceptibility SNPs.** Comparison of log Bayes factor for best
169 specific ILAR subtype model (x axis) and best shared model (y axis). Susceptibility
170 SNPs (represented by blue dots for loci from this study, red dots for previously
171 published SNPs based on oligoJIA and RF-polyJIA) above the grey line indicate
172 evidence for sharing of association across multiple ILAR subtypes.

173 **Supplementary Figure 2. Enrichment of JIA susceptibility SNPs in transcription**
174 **factor binding sites.** Annotations showing significant enrichment are displayed in
175 green.

176 **Supplementary Figure 3. Enrichment of JIA susceptibility SNPs in regulatory**
177 **regions of 98 cells.** Supplementary Table 5 provides the correspondence between cell
178 codes and cell types.

179 **Supplementary Figure 4. Enrichment of JIA susceptibility SNPs in active**
180 **promoters of 98 cells.** Supplementary Table 6 provides the correspondence between
181 cell codes and cell types.

182

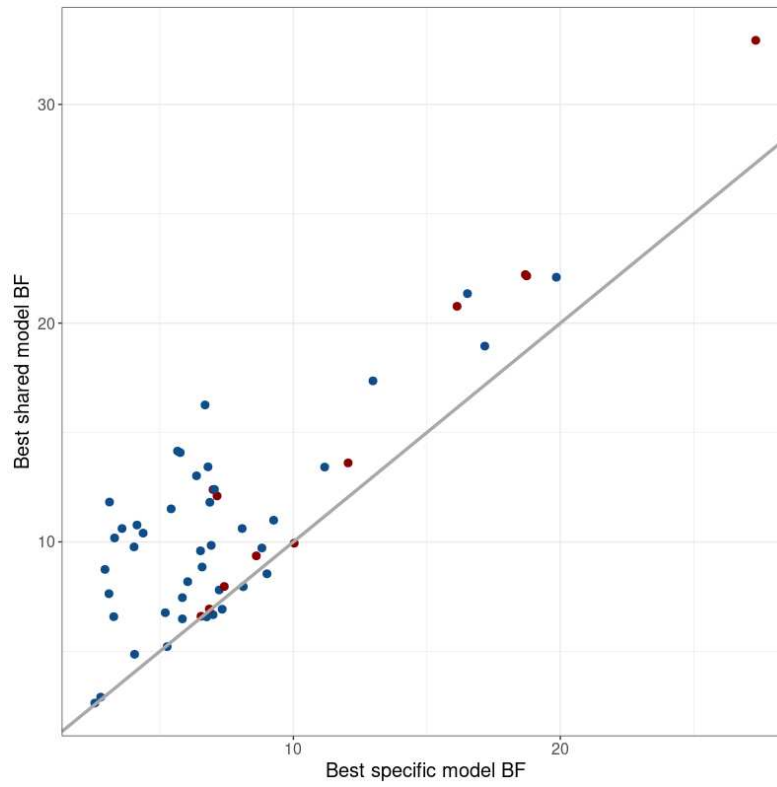
183

184 **3. SUPPLEMENTARY FIGURES**

185

186 **Supplementary Figure 1**

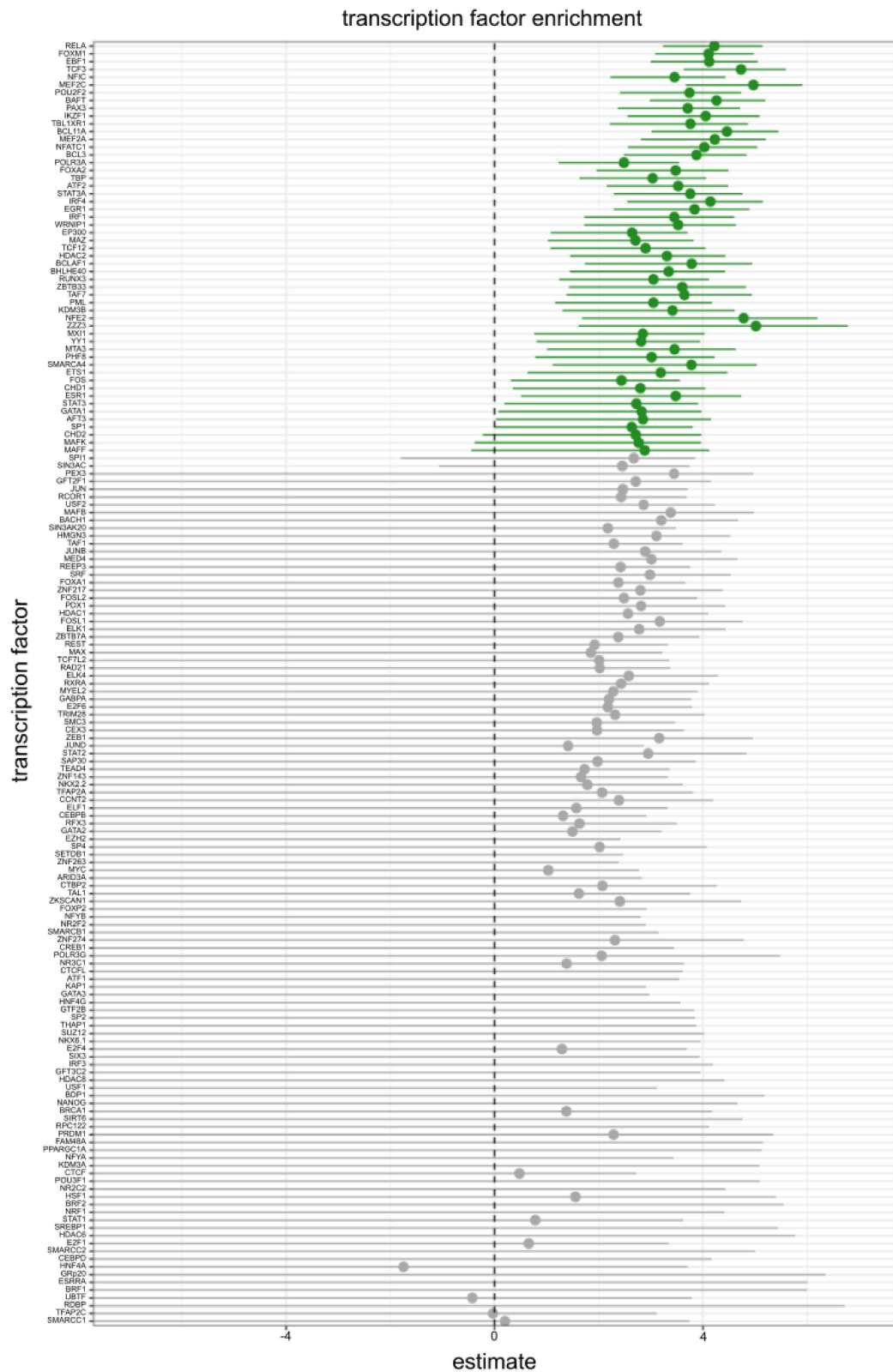
187



188

189

190 **Supplementary Figure 2**



191

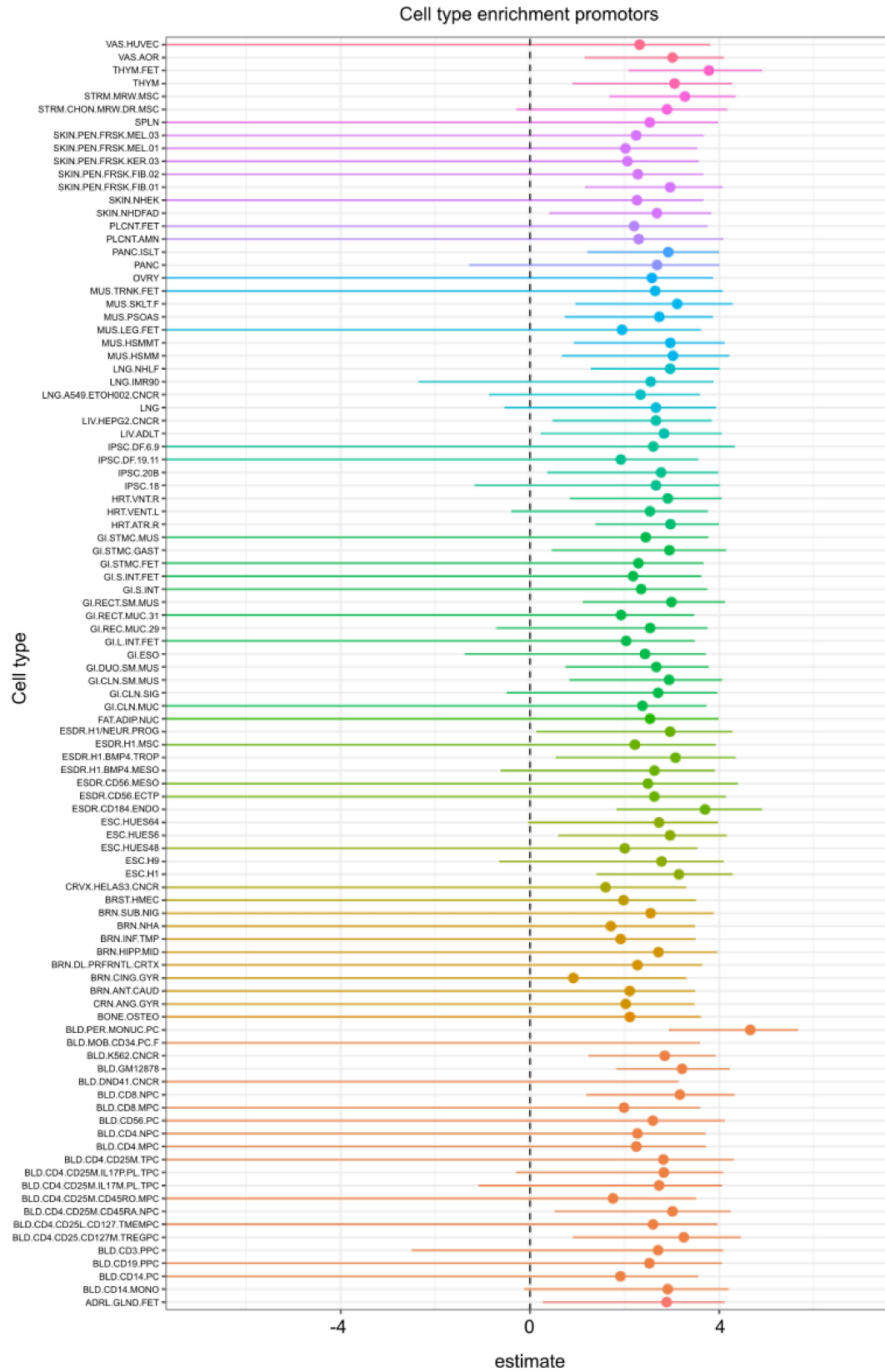
192

193 **Supplementary Figure 3**



194

195 **Supplementary Figure 4**



196

197 **4. SUPPLEMENTARY REFERENCES**

- 198 1 Packham JC, Hall MA. Long-term follow-up of 246 adults with juvenile idiopathic
199 arthritis: Functional outcome. *Rheumatology* 2002;**41**:1428–35.
200 doi:10.1093/rheumatology/41.12.1428
- 201 2 Petty RE, Southwood TR, Manners P, *et al.* International League of Associations for
202 Rheumatology classification of juvenile idiopathic arthritis: second revision,
203 Edmonton, 2001. *J Rheumatol* 2004;**31**:390–2.
- 204 3 Manichaikul A, Mychaleckyj JC, Rich SS, *et al.* Robust relationship inference in
205 genome-wide association studies. *Bioinformatics* 2010;**26**:2867–73.
206 doi:10.1093/bioinformatics/btq559
- 207 4 Abraham G, Qiu Y, Inouye M. FlashPCA2: principal component analysis of Biobank-
208 scale genotype datasets. *Bioinformatics* 2017;**33**:2776–8.
209 doi:10.1093/bioinformatics/btx299
- 210 5 Bellenguez C, Strange A, Freeman C, *et al.* A robust clustering algorithm for
211 identifying problematic samples in genome-wide association studies. *Bioinformatics*
212 2012;**28**:134–5. doi:10.1093/bioinformatics/btr599
- 213 6 McCarthy S, Das S, Kretzschmar W, *et al.* A reference panel of 64,976 haplotypes for
214 genotype imputation. *Nat Genet* 2016;**48**:1279–83. doi:10.1038/ng.3643
- 215 7 Delaneau O, Zagury JF, Marchini J. Improved whole-chromosome phasing for disease
216 and population genetic studies. *Nat Methods* 2013;**10**:5–6. doi:10.1038/nmeth.2307
- 217 8 Das S, Forer L, Schönherr S, *et al.* Next-generation genotype imputation service and
218 methods. *Nat Genet* 2016;**48**:1284–1287. doi:10.1038/ng.3656
- 219 9 McIntosh LA, Marion MC, Sudman M, *et al.* Genome-Wide Association Meta-
220 Analysis Reveals Novel Juvenile Idiopathic Arthritis Susceptibility Loci. *Arthritis*
221 *Rheumatol (Hoboken, NJ)* 2017;**69**:2222–32. doi:10.1002/art.40216
- 222 10 Magi R, Morris AP. GWAMA: software for genome-wide association meta-analysis.
223 *BMC Bioinformatics* 2010;**11**:288. doi:10.1186/1471-2105-11-288
- 224 11 Yang J, Manolio TA, Pasquale LR, *et al.* Genome partitioning of genetic variation for
225 complex traits using common SNPs. *Nat Genet* 2011;**43**:519–25. doi:10.1038/ng.823
- 226 12 Jostins L, McVean G. Trinculo: Bayesian and frequentist multinomial logistic
227 regression for genome-wide association studies of multi-category phenotypes.
228 *Bioinformatics* 2016;**32**:1898–900. doi:10.1093/bioinformatics/btw075
- 229 13 Hinks A, Cobb J, Marion MC, *et al.* Dense genotyping of immune-related disease

- 230 regions identifies 14 new susceptibility loci for juvenile idiopathic arthritis. *Nat Genet*
231 2013;**45**:664–9. doi:10.1038/ng.2614
- 232 14 Benner C, Spencer C, Havulinna AS, *et al.* FINEMAP: efficient variable selection
233 using summary data from genome-wide association studies. *Bioinformatics*
234 2016;**32**:1493–501. doi:10.1093/bioinformatics/btw018
- 235 15 Yang J, Ferreira T, Morris AP, *et al.* Conditional and joint multiple-SNP analysis of
236 GWAS summary statistics identifies additional variants influencing complex traits. *Nat*
237 *Genet* 2012;**44**:369–75, S1-3. doi:10.1038/ng.2213
- 238 16 MacArthur J, Bowler E, Cerezo M, *et al.* The new NHGRI-EBI Catalog of published
239 genome-wide association studies (GWAS Catalog). *Nucleic Acids Res* 2017;**45**:D896–
240 D901. doi:10.1093/nar/gkw1133
- 241 17 Liu X, Wu C, Li C, *et al.* dbNSFP v3.0: A One-Stop Database of Functional
242 Predictions and Annotations for Human Nonsynonymous and Splice-Site SNVs. *Hum*
243 *Mutat* 2016;**37**:235–41. doi:10.1002/humu.22932
- 244 18 Yang H, Wang K. Genomic variant annotation and prioritization with ANNOVAR and
245 wANNOVAR. *Nat Protoc* 2015;**10**:1556–66. doi:10.1038/nprot.2015.105
- 246 19 Harrow J, Frankish A, Gonzalez JM, *et al.* GENCODE: the reference human genome
247 annotation for The ENCODE Project. *Genome Res* 2012;**22**:1760–74.
248 doi:10.1101/gr.135350.111
- 249 20 ENCODE Project Consortium I, Kundaje A, Aldred SF, *et al.* An integrated
250 encyclopedia of DNA elements in the human genome. *Nature* 2012;**489**:57–74.
251 doi:10.1038/nature11247
- 252 21 Chadwick LH. The NIH Roadmap Epigenomics Program data resource. *Epigenomics*
253 2012;**4**:317–24. doi:10.2217/epi.12.18
- 254 22 Pickrell JK. Joint analysis of functional genomic data and genome-wide association
255 studies of 18 human traits. *Am J Hum Genet* 2014;**94**:559–73.
256 doi:10.1016/j.ajhg.2014.03.004
- 257 23 Schmiedel BJ, Singh D, Madrigal A, *et al.* Impact of Genetic Polymorphisms on
258 Human Immune Cell Gene Expression. *Cell* 2018;**175**:1701-1715.e16.
259 doi:10.1016/j.cell.2018.10.022
- 260 24 Giambartolomei C, Vukcevic D, Schadt EE, *et al.* Bayesian Test for Colocalisation
261 between Pairs of Genetic Association Studies Using Summary Statistics. *PLoS Genet*
262 2014;**10**:e1004383. doi:10.1371/journal.pgen.1004383
- 263 25 Mumbach MR, Satpathy AT, Boyle EA, *et al.* Enhancer connectome in primary human

- 264 cells identifies target genes of disease-associated DNA elements. *Nat Genet*
265 2017;**49**:1602–12. doi:10.1038/ng.3963
- 266 26 Chen S, Zhou Y, Chen Y, *et al.* fastp: an ultra-fast all-in-one FASTQ preprocessor.
267 *Bioinformatics* 2018;**34**:i884–90. doi:10.1093/bioinformatics/bty560
- 268 27 Servant N, Varoquaux N, Lajoie BR, *et al.* HiC-Pro: an optimized and flexible pipeline
269 for Hi-C data processing. *Genome Biol* 2015;**16**:259. doi:10.1186/s13059-015-0831-x
- 270 28 Shi C, Rattray M, Orozco G. HiChIP-Peaks: A HiChIP peak calling algorithm. *bioRxiv*
271 Published Online First: 2019. doi:10.1101/682781
- 272 29 Bhattacharyya S, Chandra V, Vijayanand P, *et al.* Identification of significant
273 chromatin contacts from HiChIP data by FitHiChIP. *Nat Commun* 2019;**10**:4221.
274 doi:10.1038/s41467-019-11950-y
- 275 30 Martin P, McGovern A, Orozco G, *et al.* Capture Hi-C reveals novel candidate genes
276 and complex long-range interactions with related autoimmune risk loci. *Nat Commun*
277 2015;**6**:10069. doi:10.1038/ncomms10069
- 278